Residual stress on the run out table accounting for multiphase transitions and transformation induced plasticity

Daniel Weisz-Patrault, Thomas Koedinger

Elsevier Editorial System(tm) for Applied Mathematical Modelling

Manuscript Draft

Manuscript Number: APM-D-17-02177

Title: Residual stress on the run out table accounting for multiphase transitions and transformation induced plasticity

Article Type: Research Paper

Keywords: Run out table, Residual stress, Eigenstrain, Multiphysics

Corresponding Author: Dr. Daniel Weisz-Patrault, Ph.D.

Corresponding Author's Institution: CNRS UMR 7649

First Author: Daniel Weisz-Patrault

Order of Authors: Daniel Weisz-Patrault; Thomas Koedinger

Abstract: The development of harder and thinner new steel grades necessitates reasonably fast numerical simulations of forming processes in order to optimize industrial conditions through parametric studies. This paper focuses on the evolution of residual stresses of thin strips during cooling on the run out table. Since the problem involves multiphysics and non-linear processes, comprehensive and fully coupled numerical approaches may be difficult to use to design or optimize industrial conditions because of extensive computation times. Therefore, a simplified numerical simulation has been developed and consists in solving first the thermal problem coupled with multiphase transitions and then the mechanical problem accounting for thermal expansion, metallurgical deformation and transformation induced plasticity. Residual stress profiles through the strip thickness are also computed in order to evaluate classic flatness defects such as crossbow and longbow. A post-processing is also included in order to quantify out of plane displacements that would take place if the strip were cut off the production line. It consists in computing at finite strain the relaxation of residual stresses when the tension applied by the coiler is released. The proposed numerical strategy has been tested on common industrial conditions.

Suggested Reviewers: Pierre Montmitonnet PhD
CEMEF, Sophia Antipolis, France, Mines de Paris, France
pierre.montmitonnet@mines-paristech.fr

Siamak Serajzadeh PhD
Department of Materials Science and Engineering, Sharif University Of Technology, Iran
serajzadeh@sharif.edu

Bernard Fedelich PhD
Department of Materials Engineering, Bundesanstalt für Materialforschung und -prüfung, Berlin, Germany
bernard.fedelich@bam.de

Dmitrii Legatiuk PhD

Faculty of Civil Engineering, Bauhaus university of Weimar, Germany
dmitrii.legatiuk@uni-weimar.de

Takayuki Otsuka PhD
Integrated Process Research Lab. , Process Research Laboratories, Nippon Steel, Japan
otsuka.6gx.takayuki@jp.nssmc.com

Cover letter:
Residual stress on the run out table accounting for multiphase transitions and transformation induced plasticity

Daniel Weisz Patrault : corresponding author

Laboratoire de Mécanique des Solides, CNRS UMR 7649, École Polytechnique, F-91128 Palaiseau, France.
Tel : (+33) 1 69 33 58 05
Email : weisz@lms.polytechnique.fr

---

1. Statement

The authors state that the submission is original and is not being submitted for publication elsewhere.

Highlights:
Residual stress on the run out table accounting for multiphase transitions and transformation induced plasticity

Daniel Weisz Patrault : corresponding author

Laboratoire de Mécanique des Solides, CNRS UMR 7649, École Polytechnique, F-91128 Palaiseau, France.
Tel : (+33) 1 69 33 58 05
Email : weisz@lms.polytechnique.fr

---

1. Highlights

- Numerical strategy to simulate a non-linear and multiphysics problem: the cooling of a steel strip on the run out table.
- Heat conduction strongly coupled with metallurgical transformations and an elastic-plastic calculation of residual stress evolution.
- Thermal expansion, density mismatch between phases and transformation induced plasticity modeled as eigenstrain.
- Significant decrease of the initial residual stress profile, but the asymmetry is responsible for bending moments
- Flatness defects such as *longbow* and *crossbow* are detected.

Residual stress on the run out table accounting for multiphase transitions and transformation induced plasticity

Daniel Weisz-Patrault*, Thomas Koedinger

LMS, École Polytechnique, CNRS, Université Paris-Saclay, 91128 Palaiseau, France

Abstract

The development of harder and thinner new steel grades necessitates reasonably fast numerical simulations of forming processes in order to optimize industrial conditions through parametric studies. This paper focuses on the evolution of residual stresses of thin strips during cooling on the run out table. Since the problem involves multiphysics and non-linear processes, comprehensive and fully coupled numerical approaches may be difficult to use to design or optimize industrial conditions because of extensive computation times. Therefore, a simplified numerical simulation has been developed and consists in solving first the thermal problem coupled with multiphase transitions and then the mechanical problem accounting for thermal expansion, metallurgical deformation and transformation induced plasticity. Residual stress profiles through the strip thickness are also computed in order to evaluate classic flatness defects such as *crossbow* and *longbow*. A post-processing is also included in order to quantify out of plane displacements that would take place if the strip were cut off the production line. It consists in computing at finite strain the relaxation of residual stresses when the tension applied by the coiler is released. The proposed numerical strategy has been tested on common industrial conditions.

Keywords: Run out table, Residual stress, Eigenstrain, Multiphysics

1. Introduction

Both the constant development of new steel grades and higher quality requirements of flat rolled products (e.g., strip thickness, strip flatness) necessitate a deep understanding of the whole chain of forming processes. Indeed, residual stresses are generated at each stage of the production line and are responsible for flatness defects. Heterogeneous plastic deformations taking place for instance during the rolling process and phase transitions occurring during

cooling on the run out table and during the coiling process (see figure 1) are the most significant contributions to the residual stress formation. Therefore, numerical simulations are needed to understand and quantify all mechanisms involved in the different processes. Thus, significant efforts have been made for the simulation of the rolling process [1, 2], the run out table [3–5] and the coiling process [6–8].

This paper focuses on the evolution of residual stresses during cooling on the run out table (after hot rolling) that is a very non linear and multiphysics process. A cooling pattern is imposed to the strip on the run out table in order to obtain a specific cooling path and phase transitions and thus a targeted microstructure may be obtained [9]. Several papers [10–15] deal with the mathematical modeling of this coupled thermal/metallurgical problem. Indeed, phase transitions are responsible for a source term in the heat conduction problem because of the enthalpy change. Most previously cited papers consider one or two-dimensional unsteady heat conduction problem solved by mixed Finite Differences for the time variable and Finite Elements for space variables. On the other hand phase transitions are computed by using the well-known Avrami's equation proposed in [16].

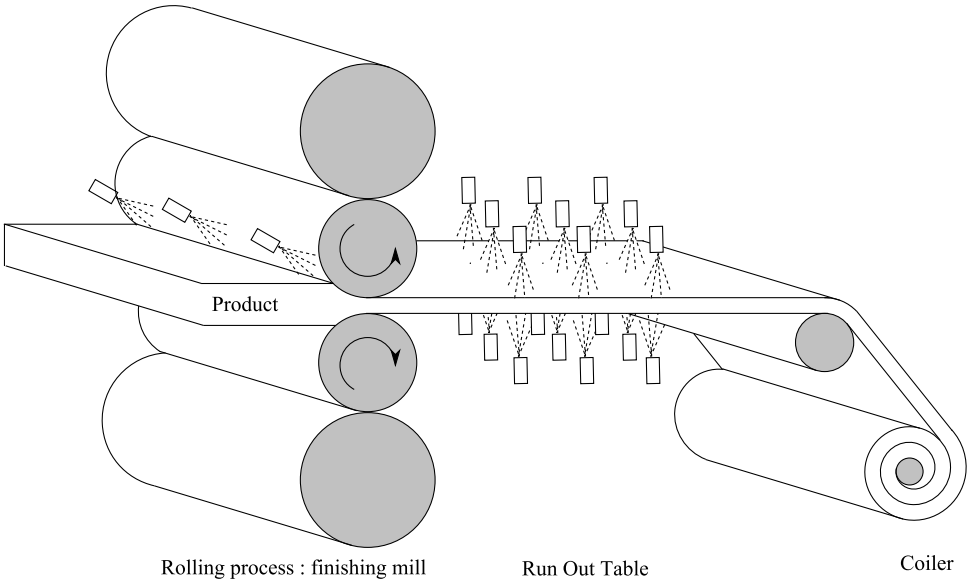

Figure 1: Chain of hot forming processes

Classic couplings between heat conduction, phase transition and mechanics are presented in figure 2. Thus, most estimations of residual stresses [17, 18, 3–5] relies on highly coupled computations even though some couplings are neglected, for instance the effect of strain and

stress on thermal and phase transition problems (dotted lines in figure 2). Despite the fact that the cited works present different degrees of details, the most common numerical strategy consists in developing a *user material* (UMAT) in the Finite Element software Abaqus [19] in order to solve simultaneously the heat conduction problem, phase transitions (via Avrami's equation) and the mechanical problem. However, the complete and fully coupled problem is very non-linear and the applicability may be limited because of very long computation times. For instance [4] can simulate a 6 meters long strip although the run out table is 130 meters long.

The present paper aims at developing a numerical strategy sufficiently fast to enable parametric studies in order to quantify in what extend industrial conditions can be adjusted to optimize flatness defects. The proposed approach relies on the very common assumption in this situation that the mechanical problem has no influence on the thermal problem and phase transitions (dotted lines in figure 2). Indeed, the problem is driven by temperature changes. Phase transitions due to mechanical deformations are negligible as well as self-heating. However, displacements obtained from the mechanical problem can be significant and affect the thermal/metallurgical problem, principally when instabilities occur if mechanical computations are done at finite strain. In this contribution, computations are done under infinitesimal strain assumption and then the effect of geometry changes (on the thermal/metallurgical problem) is neglected. Thus, two numerical calculations can be conducted successively, first the coupled thermal/metallurgical problem and then the mechanical problem. This approach enables us to use different numerical schemes and different geometrical descriptions for each one of the two problems.

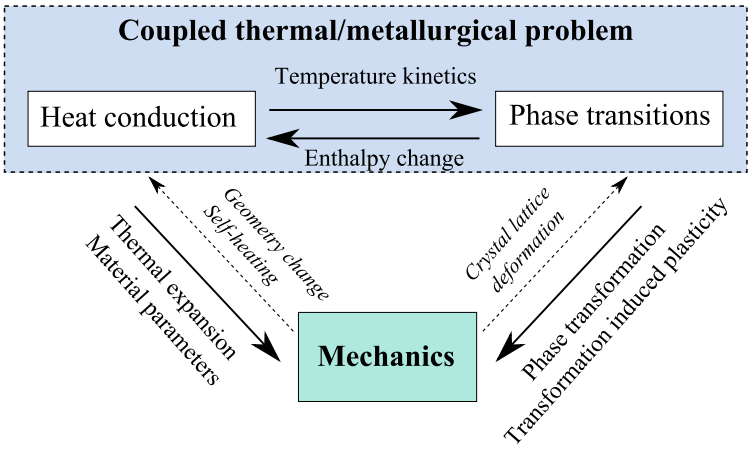

Figure 2: Couplings

The global numerical scheme is divided into three different numerical items. First the coupled thermal/metallurgical problem is solved by using TACSI proposed in [20–22]. Thus, temperature and phase proportion fields are extracted at each time step. Thermal expansion, density mismatch between phases and transformation induced plasticity are combined in the form of an eigenstrain increment that is computed by using the free software SCILAB [23]. This eigenstrain being incompatible in general (i.e., it cannot be written as the gradient of a displacement field) an elastic strain should be introduced so that the total strain is compatible. This mechanical problem is solved by using the Finite Element software CAST3M [24].

The paper is constructed as follows. The global numerical strategy is detailed in section 2. Calculation of the eigenstrain increment is then broached in section 3. In particular transformation induced plasticity is discussed. The mechanical problem of a strip subjected to the eigenstrain increment is then addressed in section 4. Material parameters are extracted from the literature as a function of temperature and representative run out table conditions are selected in section 5.1. Numerical computations are presented and analyzed in section 5.2. A post-processing is also included in section 6 in order to quantify the flatness defect that would take place if the strip were cut off the production line. It consists in computing at finite strain the relaxation of residual stress when the tension applied by the coiler is released. Conclusive remarks are proposed in section 7.

2. Numerical strategy

The global numerical scheme proposed in this paper is summarized in figure 3. The general problem of the strip cooling down on the run out table is divided into three numerical tasks.

1) The first task consists in solving the coupled heat conduction problem with phase transitions by using TACSI proposed in [20–22]. This program is based on the unsteady heat equation with source terms due to enthalpy changes (phase transitions) given by:

$$\mathrm{div}\,(\lambda(T)\boldsymbol{\nabla}T) - \rho(T)c_p\frac{\partial T}{\partial t} = -\sum_{p=2}^{N_p}\Delta H_p(T)\dot{X}_p \tag{1}$$

where T denotes the temperature, $\lambda(T)$ the thermal conductivity, $\rho(T)$ the density of the multiphase mixture, c_p the thermal capacity, $\Delta H_p(T)$ the enthalpy change during phase transformation, X_p the phase proportion of p-th phase and N_p the number of considered

phases. Time dependent boundary conditions are imposed through various Heat Transfer Coefficients that describe the known process conditions (water cooling, wet and dry zones). TACSI relies on solving (1) in 1D along the strip thickness. That is to say that a material particle (described by a segment along the strip thickness) is cooled down by moving to the run out table. Explicit Finite Differences are used and the coupling procedure consists in alternating at each time step the heat conduction solver and the phase transition solver. Phase transitions are most of the time described by Avrami's equation that relies on statistical treatments and assumptions (e.g., pre-existence of germ nuclei of the product phase with a certain probability of growth) and predicts the overall transformation kinetics for diffusive transformations under isothermal assumption. For non-isothermal conditions, the so-called isokinetic assumption has been extended in [25] leading to a modified equation. This approach is accurate but relies on experimental identifications that should be done for each tested grade. Physical approaches on the other hand, do not require a full experimental fitting procedure for each grade. Nucleation and growth models have been been proposed as reviewed for instance in [26]. The phase transition model included in TACSI relies on such a physical modeling. The nucleation and growth are modeled by thermodynamical and kinetics approaches. For details the reader is refereed to [20].

At each time step a coupling with phase transitions is computed and the temperature and phase proportion fields are computed at three positions through the strip thickness (upper and lower surface and mid-plane). Moreover, a steady state is assumed on the run out table, that is to say that the global temperature field does not vary along the strip length even though each material particle undergoes very rapid thermal and structural evolutions. Since neither the geometrical strip profile (obtained during the rolling process) nor the cooling conditions on the run out table are perfectly constant, no steady state is never strictly reached. However, temperature and phase proportion fields evolve much slower than the strip speed. Therefore, one can assume that by selecting several points along the strip width at one particular position along the strip length, one can construct temperature and phase proportion fields for a strip portion as long as the the run out table. This simplified approach enables us to compute effectively the whole temperature and phase proportion fields just by computing the evolution uni-dimensional material particles (at different position along the strip width) moving to the run out table.

2) The second task consists in computing for each time step the eigenstrain increment (denoted by $\Delta\boldsymbol{\varepsilon}_k^*$ where k refers to the time increment) accounting for thermal expansion, phase transformations and transformation induced plasticity. To that end a numerical code has been written by using the free software SCILAB [23].

3) The third task consists in solving at each time step the elastic-plastic problem of the strip undergoing the eigenstrain increment $\Delta\boldsymbol{\varepsilon}_k^*$ by using the Finite Element software CAST3M [24]. Indeed, the eigenstrain is not the gradient of a displacement field and an elastic strain should be introduced so that the total strain is compatible. A global plastic strain is also considered in the total strain because the eigenstrain increment can be sufficient to generated macroscopic plasticity. Moreover an initial residual stress profile (obtained at the end of the rolling process) is considered and the traction applied by the coiler is also taken into account. Finite Element computations are done under infinitesimal strain assumption by using quadrangular shell elements in order to obtain short computation times.

It should be noted that the mechanical problem depends on the loading path both because of the fact that the eigenstrain increment depends on the stress state of the previous time step and because of the elastic-plastic behavior. Thus, one cannot compute directly the mechanical problem from the temperature and phase proportion fields obtained on the run out table. Strain and stress *history* should be considered by applying progressively the temperature and phase proportion fields responsible for the eigenstrain as shown in figure 4. As a result, several FE computations are performed alternatively with computations of the eigenstrain increments.

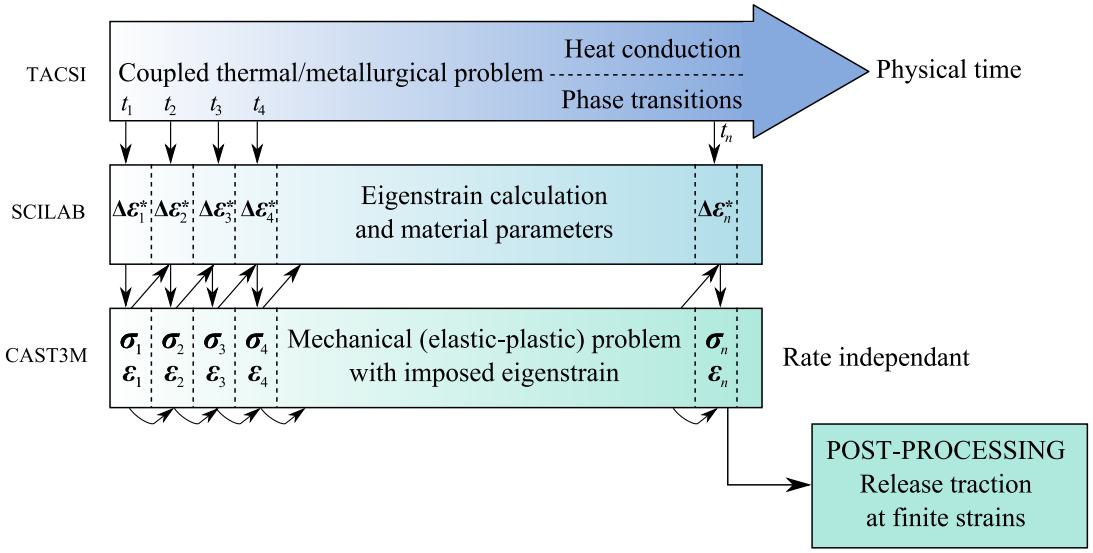

Figure 3: Numerical scheme

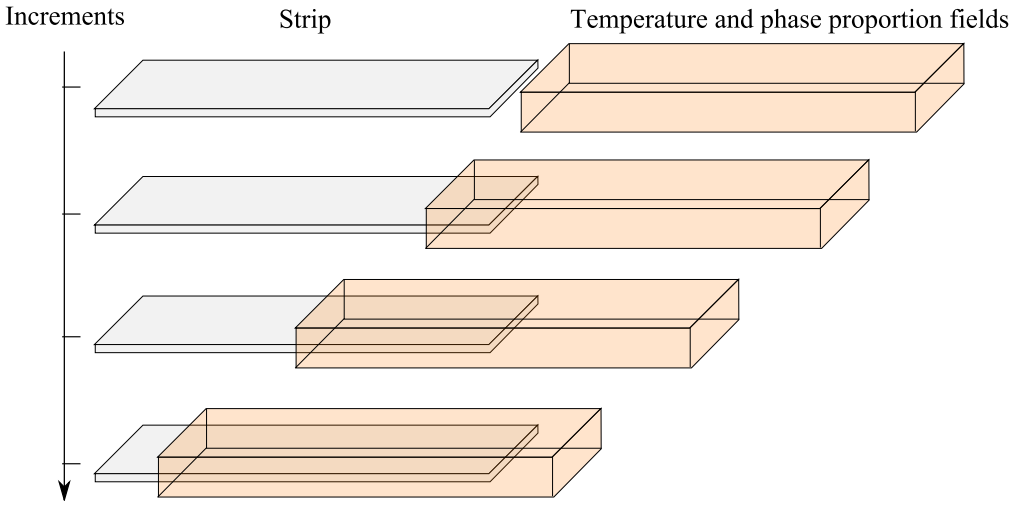

Figure 4: History of mechanical states

3. Eigenstrain and transformation induced plasticity

During cooling on the run out table significant temperature and structural changes take place under mechanical loads (applied tension by the coiler and initial residual stresses). Thus, the strip undergoes thermal expansion, phase transformation and transformation induced plasticity. Indeed, when phase transformations occur under applied mechanical loads that can be much lower than the yield stress, significant plastic strains are observed. This phenomenon called

transformation induced plasticity or sometimes super-plasticity received particular attention. The Leblond's model proposed in [27–30] is one of the most fruitful model for industrial implementation. Indeed, because of its solid theoretical basis and the fact that the overall transformation induced plastic strain increment is given by simple explicit formulas, the Leblond's model has been intensively used for various engineering applications and especially for run out table simulations. For instance [4] used a slightly improved version of the Leblond's model proposed in [31]. Within the framework of run out table simulations, a simple formulation for transformation induced plasticity has also been proposed in [32]. However, there is no theoretical derivation from previous mechanical knowledge and the proposed formula is an Arrhenius equation to be fitted with experimental data. This approach has been used for instance in [17].

Most transformation induced plasticity models are dedicated to simple two-phases mixtures. However, multiphase transitions occur in steel during cooling. Residual austenite may be transformed into ferrite, pearlite, bainite and martensite depending on the local temperature kinetics. An attempt to extend the Leblond's model to multiphase transitions has been proposed in [33] but formulas are adapted without theoretical developments as originally made in the Leblond's model. In this paper transformation induced plasticity and classic plasticity related to temperature and stress variations are computed following the recent theoretical work [34] that extends properly the original Leblond's model. Multiphase transitions are taken into account and several assumptions in the original work are relaxed.

Main results useful for this paper are recalled for sake of clarity. It should be noted that expressions are particularized for this study, that is to say during cooling only and for the following phase transitions austenite to ferrite, austenite to pearlite, austenite to bainite and austenite to martensite. For more general equations, the reader is refereed to [34]. At each time step k, the elastic-plastic problem consists in solving the following equation:

$$\begin{cases} \mathbf{div}\left(\boldsymbol{\sigma}_k\right) = 0 & \text{Equilibrium} \\ \boldsymbol{\sigma}_k = \lambda(T_k)\mathrm{tr}\left(\boldsymbol{\varepsilon}_k^e\right)\boldsymbol{I} + 2\mu(T_k)\boldsymbol{\varepsilon}_k^e & \text{Isotropic behavior} \\ \boldsymbol{\varepsilon}_k = \frac{1}{2}\left(\boldsymbol{\nabla} \boldsymbol{u}_k + \boldsymbol{\nabla} \boldsymbol{u}_k^T\right) & \text{Compatibility} \\ \boldsymbol{\varepsilon}_k = \boldsymbol{\varepsilon}_k^e + \boldsymbol{\varepsilon}_k^p + \boldsymbol{\varepsilon}_{k-1} + \Delta\boldsymbol{\varepsilon}_k^* & \text{Total strain tensor} \end{cases} \tag{2}$$

T_k is the temperature field at the k-th increment and $\lambda(T_k)$ and $\mu(T_k)$ are the temperature dependent Lamé's coefficients of the multiphase mixture. In this paper, a simple mixture rule is

chosen:

$$\lambda(T_k) = \sum_{p=1}^{N_p} X_{p,k}\lambda_p(T_k) \quad \text{and} \quad \mu(T_k) = \sum_{p=1}^{N_p} X_{p,k}\mu_p(T_k) \tag{3}$$

Where λ_p and μ_p are the Lamé's coefficients of phase p and $X_{p,k}$ denote the phase proportion of phase p and N_p is the number of considered phases ($p = 1$: austenite, $p = 2$: ferrite, $p = 3$: pearlite, $p = 4$: bainite and $p = 5$: martensite). Moreover, $\boldsymbol{u}$ denotes the displacement vector, $\boldsymbol{\sigma}_k$ is the Cauchy stress tensor, $\boldsymbol{\varepsilon}_k$ and $\boldsymbol{\varepsilon}_{k-1}$ denote the total strain at the k-th and $(k-1)$-th increments respectively and $\boldsymbol{\varepsilon}^e$ and $\boldsymbol{\varepsilon}^p$ denote the unknown elastic and plastic strain respectively. It should be noted that the initial residual stress profile can be either set with an initial stress field $\boldsymbol{\sigma}_0$ in CAST3M or by imposing that $\boldsymbol{\varepsilon}_0$ corresponds to the elastic counter part of the initial residual stress profile.

In addition, $\Delta\boldsymbol{\varepsilon}^*_k$ denotes the eigenstrain increment introduced because of thermal expansion, phase transitions and transformation induced plasticity associated with increment of temperature ΔT_k and increment of phase proportion $\Delta X_{p,k}$. The eigenstrain increment $\Delta\boldsymbol{\varepsilon}^*_k$ can be decomposed as follows:

$$\Delta\boldsymbol{\varepsilon}^*_k = \Delta\boldsymbol{\varepsilon}^{thm}_k + \Delta\boldsymbol{\varepsilon}^{tp}_k + \Delta\boldsymbol{\varepsilon}^{cp}_{T,k} + \Delta\boldsymbol{\varepsilon}^{cp}_{\boldsymbol{\sigma},k} \tag{4}$$

Where $\Delta\boldsymbol{\varepsilon}^{thm}_k$ denotes the thermo-metallurgical strain tensor, which corresponds to volume variations due to thermal dilatation and density mismatch between phases, $\Delta\boldsymbol{\varepsilon}^{tp}_k$ is the transformation induced plasticity tensor and $\Delta\boldsymbol{\varepsilon}^{cp}_{\boldsymbol{\sigma},k}$ and $\Delta\boldsymbol{\varepsilon}^{cp}_{T,k}$ are the classic plasticity tensors induced by equivalent stress and temperature variations respectively. The contribution of $\Delta\boldsymbol{\varepsilon}^{cp}_{\boldsymbol{\sigma},k}$ is neglected.

After [34], the hydrostatic thermo-metallurgical strain increment is shown to be:

$$\Delta\boldsymbol{\varepsilon}^{thm} = \sum_{p=2}^{N_p} \frac{1}{3}\left(\frac{\rho_1(T_k)}{\rho_p(T_k)} - 1\right)\Delta X_{p,k} + \left(\alpha_1 + \sum_{p=2}^{N_p} X_{p,k}(\alpha_p - \alpha_1)\right)\Delta T_k \tag{5}$$

Where ρ_p is the density of phase p and α_p is the thermal expansion coefficient of phase p. Consider $\widetilde{X}_k$ the total product phase proportion:

$$\widetilde{X}_k = 1 - X_{1,k} = \sum_{p=2}^{N_p} X_{p,k} \tag{6}$$

and $\Delta\sigma^Y$ the following quantity:

$$\Delta\sigma^Y = \sqrt{\left(\sigma_1^Y\right)^2 - \left(\sigma_1^{eq}\right)^2} \tag{7}$$

where σ_p^Y is the yield stress, σ_p^{eq} the von Mises equivalent stress and ε_p^{eq} the von Mises equivalent plastic strain in phase p. Consider the following material parameters:

$$\begin{cases} \zeta = \dfrac{(3\lambda_1 + 2\mu_1)2\mu_1}{\lambda_1 + 2\mu_1} \\ \xi_p = \dfrac{2\mu_1(9\lambda_1 + 14\mu_1)}{\lambda_1(9\mu_1 + 6\mu_p) + 2\mu_1(7\mu_1 + 8\mu_p)} \end{cases} \tag{8}$$

The transformation plastic strain increment reads if $\sigma_1^{eq} < \sigma_1^Y$:

$$\Delta\boldsymbol{\varepsilon}^{tp} = \sum_{p=2}^{N_p} \frac{\boldsymbol{s}_{p,k}}{\sigma_p^Y} \frac{\sigma_p^Y - \sigma_p^{eq}}{\mu_p \xi_p} \Delta X_{p,k} + \begin{cases} 0 & \text{if} \quad \dfrac{\Delta\sigma^Y}{\zeta \left|\widetilde{\varepsilon}^{thm}\right|} > 1 \\ -\dfrac{3\left|\widetilde{\varepsilon}^{thm}\right| \boldsymbol{s}_{1,k}}{\sigma_1^Y(\varepsilon_1^{eq})} \ln\left(\dfrac{\Delta\sigma^Y}{\zeta \left|\widetilde{\varepsilon}^{thm}\right|}\right) \displaystyle\sum_{\substack{p=2 \\ \Delta X_{p,k}>0}}^{N_p} \Delta X_{p,k} & \text{if} \quad \widetilde{X}_k \leq \dfrac{\Delta\sigma^Y}{\zeta \left|\widetilde{\varepsilon}^{thm}\right|} \leq 1 \\ -\dfrac{3\left|\widetilde{\varepsilon}^{thm}\right| \boldsymbol{s}_{1,k}}{\sigma_1^Y(\varepsilon_1^{eq})} \ln\left(\widetilde{X}_k\right) \displaystyle\sum_{\substack{p=2 \\ \Delta X_{p,k}>0}}^{N_p} \Delta X_{p,k} & \text{if} \quad \widetilde{X}_k > \dfrac{\Delta\sigma^Y}{\zeta \left|\widetilde{\varepsilon}^{thm}\right|} \end{cases} \tag{9}$$

Where $\boldsymbol{s}_{p,k}$ is the deviatoric stress tensor of phase p. And if $\sigma_1^{eq} = \sigma_1^Y$:

$$\Delta\boldsymbol{\varepsilon}^{tp} = \sum_{p=2}^{N_p} \frac{\boldsymbol{s}_{p,k}}{\sigma_p^Y} \frac{\sigma_p^Y - \sigma_p^{eq}}{\mu_p \xi_p} \Delta X_{p,k} + \begin{cases} 0 & \text{if} \quad \widetilde{X}_k < \widetilde{X}_{min} \\ -\dfrac{3\left|\widetilde{\varepsilon}^{thm}\right| \boldsymbol{s}_{1,k}}{\sigma_1^Y} \ln\left(\widetilde{X}_k\right) \displaystyle\sum_{\substack{p=2 \\ \Delta X_{p,k}>0}}^{N_p} \Delta X_{p,k} & \text{if} \quad \widetilde{X}_k \geq \widetilde{X}_{min} \end{cases} \tag{10}$$

with the initial value:

$$\boldsymbol{\varepsilon}_{ini}^{tp} = \frac{2\widetilde{\varepsilon}^{thm}}{1 - \widetilde{X}_{min}} \widetilde{X}_{min} \ln\left(\widetilde{X}_{min}\right) \tag{11}$$

where $\widetilde{X}_{min}$ (set to 0.03 in this paper) is the minimal phase proportion that can be produced from pure austenite and where $\widetilde{\varepsilon}^{thm}$ is the hydrostatic eigenstrain generated in all product phases because of temperature variation and phase transitions:

$$\widetilde{\varepsilon}^{thm} = \sum_{p=2}^{N_p} \frac{X_{p,k}}{1 - X_1} \left(\frac{1}{3} \left(\frac{\rho_1(T_k)}{\rho_p(T_k)} - 1 \right) + \frac{\rho_1(T_k)}{\rho_p(T_k)} (\alpha_p - \alpha_1)(T_k - T_{ini}) \right) > 0 \tag{12}$$

It should be mentioned that $\widetilde{\varepsilon}^{thm}$ given by (12) is related to the microstructure and should not be mixed up with the homogenized hydrostatic strain $\boldsymbol{\varepsilon}^{thm}$ given by (5). The classic plastic strain

rate due to thermal variations reads if $\sigma_1^{eq} < \sigma_1^Y$:

$$\Delta\boldsymbol{\varepsilon}_T^{cp} = \begin{cases} 0 & \text{if} \quad \dfrac{\Delta\sigma^Y}{\zeta\left|\widetilde{\varepsilon}^{thm}\right|} > 1 \\ \dfrac{-3\widetilde{\alpha}\boldsymbol{s}_{1,k}}{\sigma_1^Y(\varepsilon_1^{eq})}\widetilde{X}_k \ln\left(\dfrac{\Delta\sigma^Y}{\zeta\left|\widetilde{\varepsilon}^{thm}\right|}\right)\Delta T_k & \text{if} \quad \widetilde{X}_k \leq \dfrac{\Delta\sigma^Y}{\zeta\left|\widetilde{\varepsilon}^{thm}\right|} \leq 1 \\ \dfrac{-3\widetilde{\alpha}\boldsymbol{s}_{1,k}}{\sigma_1^Y(\varepsilon_1^{eq})}\widetilde{X}_k \ln\left(\widetilde{X}_k\right)\Delta T_k & \text{if} \quad \widetilde{X}_k > \dfrac{\Delta\sigma^Y}{\zeta\left|\widetilde{\varepsilon}^{thm}\right|} \end{cases} \tag{13}$$

And if $\sigma_1^{eq} = \sigma_1^Y$:

$$\Delta\boldsymbol{\varepsilon}_T^{cp} = \frac{-3\widetilde{\alpha}\boldsymbol{s}_{1,k}}{\sigma_1^Y}\widetilde{X}_k \ln\left(\widetilde{X}_k\right)\Delta T_k \tag{14}$$

where $\widetilde{\alpha}$ represents the homogenized difference between thermal expansion coefficient in the product phases and in the austenite:

$$\widetilde{\alpha} = \sum_{p=2}^{N_p} \frac{X_{p,k}}{1 - X_1}\left(\alpha_p - \alpha_1\right) < 0 \tag{15}$$

4. Elastic-plastic problem with imposed eigenstrain

4.1. Generalized stess and strain

Equation (2) is solved at each time step under infinitesimal strain assumption, by using the Finite Element free software CAST3M. Quadrangular linear shell element `'COQ4'` is used in order to obtain short computation times. Consider Cartesian coordinates (x_1, x_2, x_3) corresponding respectively to the direction of strip length, strip width and strip thickness. There are 5 generalized kinematic unknowns (degrees of freedom) for this element: three translations U_1, U_2, U_3 and two rotations φ_1, φ_2. Moreover the mechanical state relies on 8 generalized stress components. Thus the in-plane stress resultants $\boldsymbol{N}$, bending moments $\boldsymbol{M}$ and shear resultants $\boldsymbol{Q}$ are defined as follows:

$$\forall (i,j) \in \{1,2\}^2, \begin{cases} N_{ij} = \displaystyle\int_{-\frac{h}{2}}^{\frac{h}{2}} \sigma_{ij} \mathrm{d}x_3 \\ M_{ij} = \displaystyle\int_{-\frac{h}{2}}^{\frac{h}{2}} x_3\sigma_{ij} \mathrm{d}x_3 \\ Q_i = \displaystyle\int_{-\frac{h}{2}}^{\frac{h}{2}} \sigma_{i3} \mathrm{d}x_3 \end{cases} \tag{16}$$

where h is the strip thickness that depends on x_2 because of the strip geometrical profile. From the computed quantities N_{ij}, M_{ij}, Q_i using the FE computation, one should compute an estima-

tion of three dimensional Cauchy stresses in order to compute the imposed eigenstrain increment $\Delta\boldsymbol{\varepsilon}^*$ for the next time step (as detailed in section 3). By assuming a linear dependence on the thickness direction x_3 for σ_{ij} and homogenous σ_{i3} (for $(i,j) \in \{1,2\}^2$) one obtains:

$$\forall (i,j) \in \{1,2\}^2, \quad \begin{cases} \sigma_{ij} = \dfrac{12M_{ij}}{h^3}x_3 + \dfrac{N_{ij}}{h} \\ \sigma_{i3} = \dfrac{Q_i}{h} \end{cases} \quad \text{and} \quad \sigma_{33} = 0 \tag{17}$$

The generalized eigenstrain to be imposed in the FE model, is constituted of 8 components (plane and shear eigenstrain and curvature) denoted by $\Delta E^*_{ij}, \Delta G^*_{i3}, \Delta R^*_{ij}$. This generalized eigenstrain is given as a function of the three dimensional eigenstrain computed following section 3 as follows:

$$\forall (i,j) \in \{1,2\}^2, \begin{cases} \Delta E^*_{ij} = \dfrac{1}{h}\displaystyle\int_{-\frac{h}{2}}^{\frac{h}{2}} \Delta\varepsilon^*_{ij}\mathrm{d}x_3 \\ \Delta G^*_{i3} = \dfrac{1}{h}\displaystyle\int_{-\frac{h}{2}}^{\frac{h}{2}} \Delta\varepsilon^*_{i3}\mathrm{d}x_3 \\ \Delta R^*_{ij} = \dfrac{12}{h^3}\displaystyle\int_{-\frac{h}{2}}^{\frac{h}{2}} x_3\Delta\varepsilon^*_{ij}\mathrm{d}x_3 \end{cases} \tag{18}$$

4.2. Boundary conditions

Boundary conditions are specified as follows. At one end of the strip an average tension is applied by the coiler and displacement U_3 is blocked. Furthermore, displacements U_1 and U_3 and all rotations are blocked at the other end. However, edge effects should be avoided. Indeed, the local distribution of the applied tension is unknown, only the resultant force applied by the coiler is known. Similarly, displacements are not blocked at the other end but a distribution takes place instead. This difficulty is overcome by adding extra pieces of strip (whose length is twice the strip width) at both ends of the strip in order to apply boundary conditions. Thus, mechanical fields unduly affected by simplified boundary conditions does not spread in the real zone of interest. It should be mentioned that in the following results are presented only in this zone of interest.

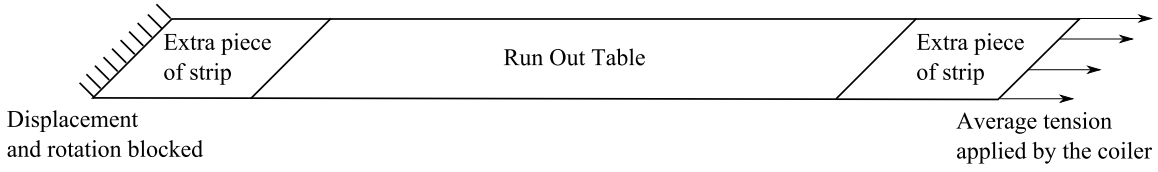

Figure 5: Boundary conditions

5. Numerical simulation

5.1. Material parameters and modeling conditions

A numerical example is proposed in order to present typical outputs of the model. A 140 m long run out table is considered. A steel strip initially at 1150 K and going at 10.25 m/s is cooled down on the run out table with water-jets identically distributed along the strip width. The cooling path along the strip length is determined by a succession of water, wet and dry zones characterized by Heat Transfer Coefficients. The upper surface is cooled down faster than the lower surface because there are more water jets spraying on the upper surface, as shown in figure 6. The geometrical profile defines the strip thickness as a quadratic function of the strip width (i.e., x_2 coordinate). In this example, a 3 mm thick strip is considered with a strip crown of 2% (i.e., the strip thickness at the edges is 98 % of the strip thickness at the center). The temperature and phase proportion fields are presented in figure 7a and 7b at three positions along the strip thickness (top, middle and bottom). There are almost no variations along the strip width because the cooling is homogeneous along this direction. However it is clear that the upper surface is cooled down faster than the lower surface. Material parameters are extracted from the literature. The Poisson coefficient is set to 0.3 and the Young modulus is assumed to be identical for all phases and given by [35]:

$$E(T) = 2.08 \times 10^5 - 1.90 \times 10^2 T + 1.19 T^2 - 2.82 \times 10^{-3} T^3 + 1.66 \times 10^{-6} T^4 \qquad (19)$$

On the other hands, temperature dependent yield stresses are given for each phase in figure 8a by interpolating numerical values found in [36].

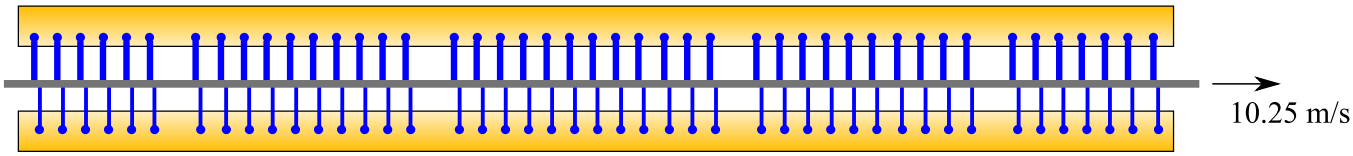

Figure 6: Prescribed cooling path

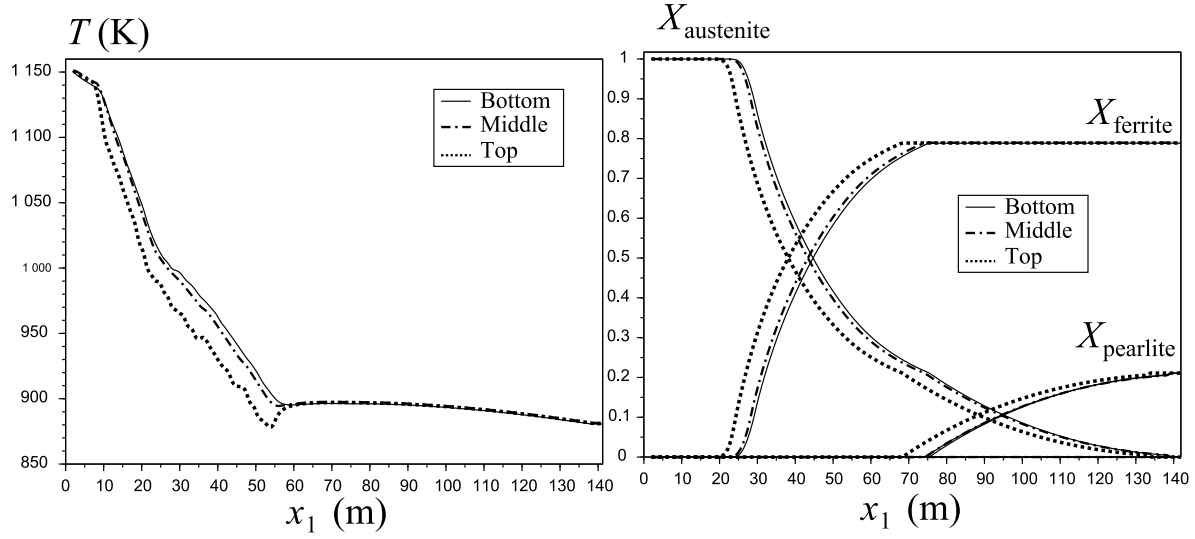

(a) Temperature field

(b) Phase proportion field

Figure 7: Coupled thermal/metallurgical problem

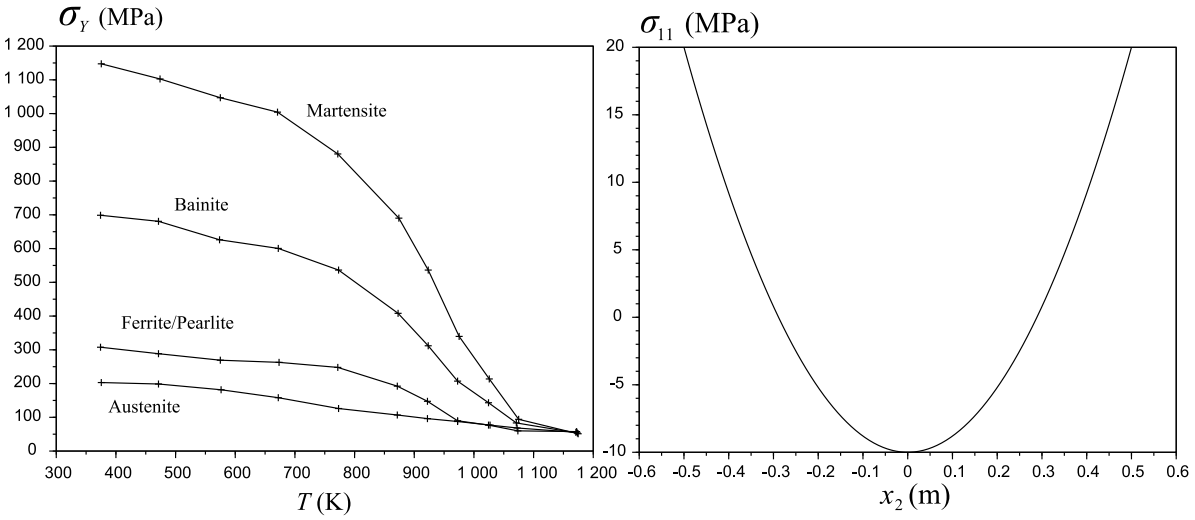

(a) Yield stress of each phase

(b) Initial residual stress profile

Furthermore, an initial residual stress profile is considered in this numerical simulation. A simple variation of σ_{11} along the strip width is presented in figure 8b. There is no variation of the initial residual stress profile along the strip thickness in this numerical example. The strip is modeled in CAST3M with 10 elements along the strip width and 560 elements along the strip length.

5.2. Results

Numerical results are given at different time steps for the in-plane stress resultant N_{11} and the bending moment M_{11} in figure 9 and 10. Six other components are calculated but for sake of concision only the most interesting components are presented. The effect of plasticity and transformation induced plasticity is clearly in this example to reduce significantly the residual stress state. This is due to the fact that temperature and phase proportion fields are almost homogenous along the strip width. However, since the cooling path is not symmetric (upper surface cooled down faster than the lower surface), bending moments are generated. It can be noticed that there is a maximum zone in figure 10 that shifts according to time steps. This is only due to the equilibrium because of the quick variation of the in-plane stress resultant N_{11}.

The final residual stress profile, that takes place in the strip, is obtained at the last time step at the end of the run out table. Stresses at three positions along the strip thickness are presented in figure 11 as well as the corresponding bending moments. Therefore by comparing initial and final residual stress profiles in figure 8b and 11 , it is clear with the proposed simulation parameters (e.g., cooling path is homogenous along the strip width) that plasticity tends to decrease significantly the stress level. However, bending moments are also introduced and are responsible for flatness defects called *longbow* and *crossbow*. It should be noted that the resultant of σ_{11} has been subtracted in figure 11a in order to remove the offset due to the applied tension even though at this stage there is no computation of the the residual stress relaxation by properly releasing the tension.

The entire simulation lasts aroud 2 hours and a non-negligible part of the computation time is used for writing files characterizing the mechanical state in order to compute the increment of eigenstrain. Thus, a way of reducing even more computation times is to avoid to write these files by using the flash memory instead.

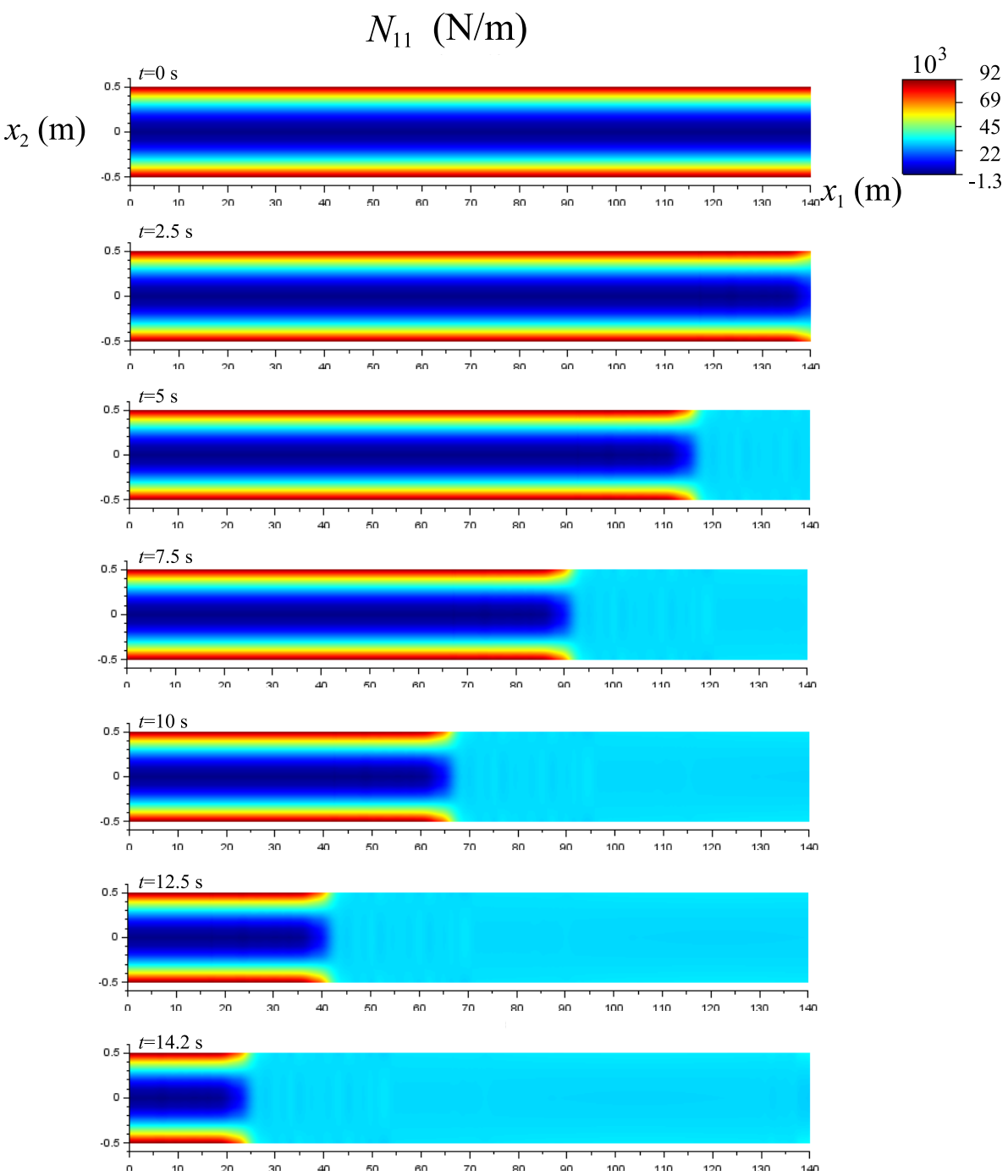

Figure 9: In-plane stress resultant N_{11}

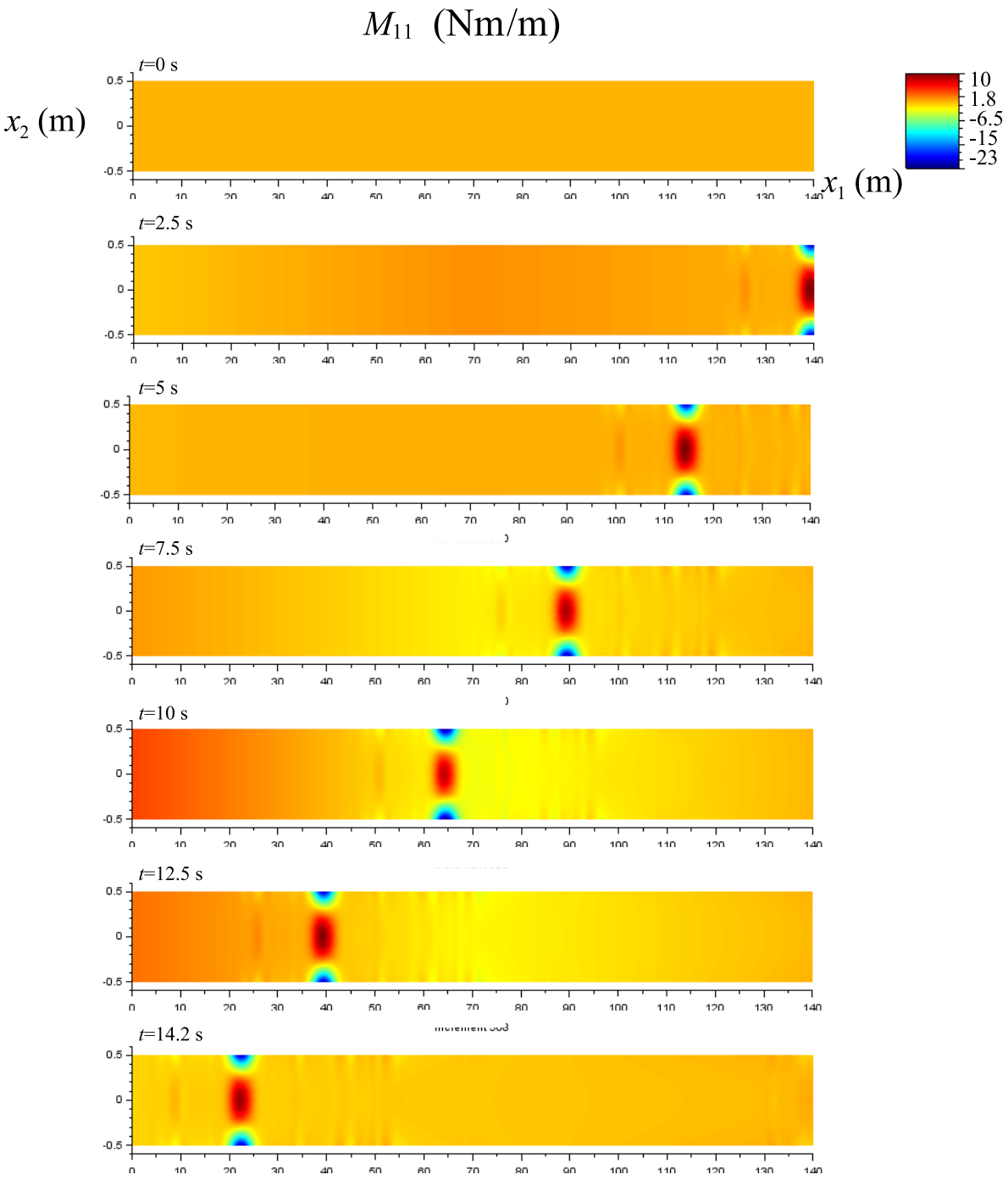

Figure 10: Bending moment M_{11}

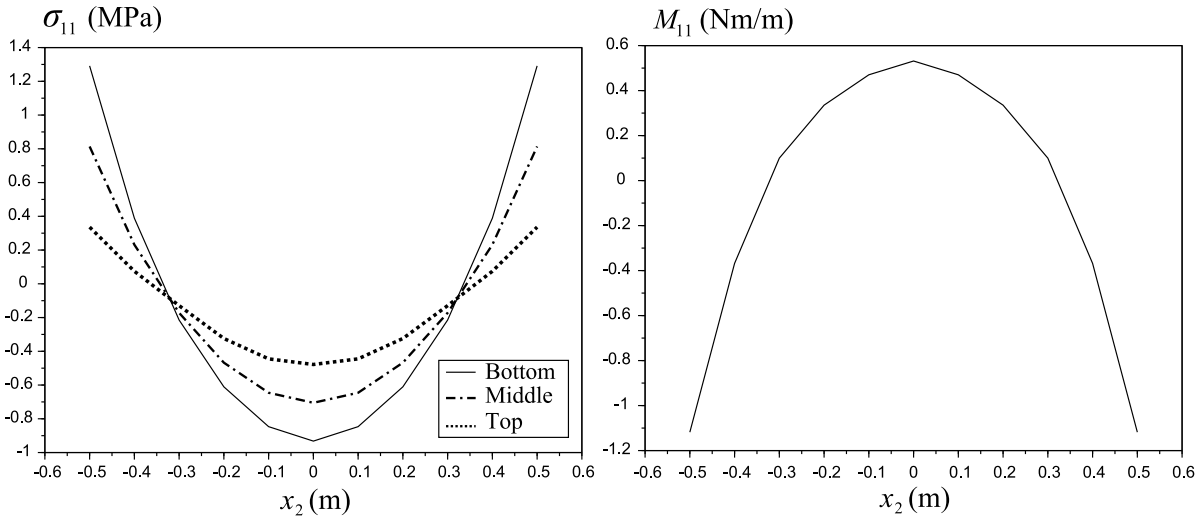

(a) Final residual stress σ_{11}

(b) Final bending moment M_{11}

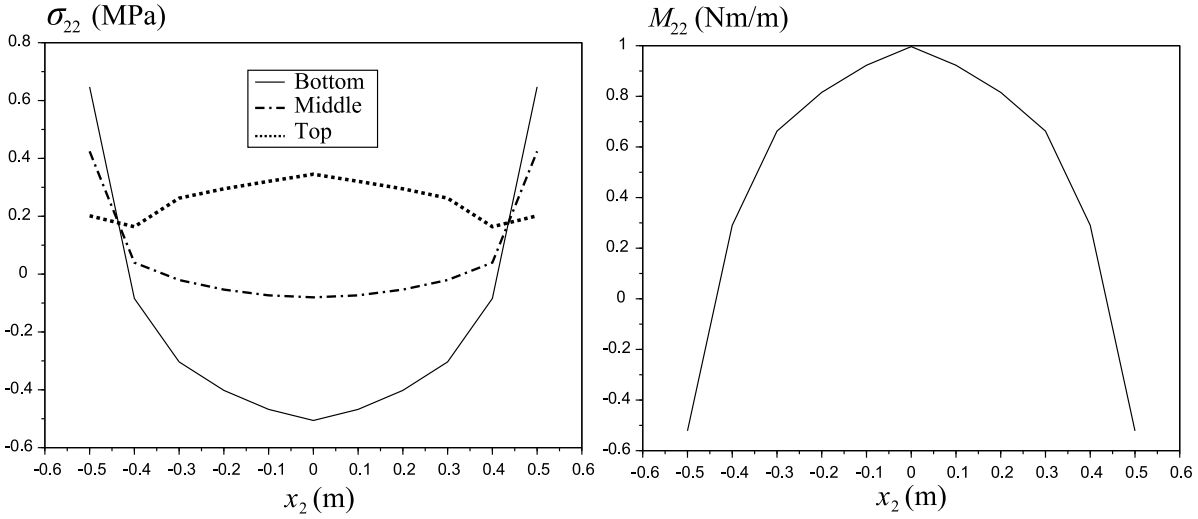

(c) Final residual stress σ_{22}

(d) Final bending moment M_{22}

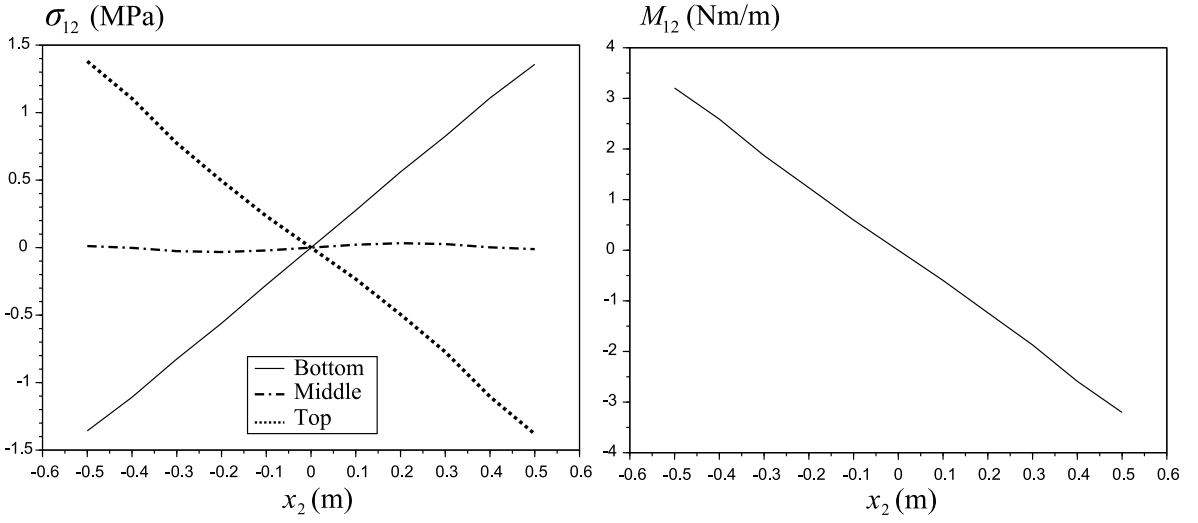

(e) Final residual stress σ_{12}

(f) Final bending moment M_{12}

Figure 11: Final stress profiles

6. Relaxation of residual stresses

In this section a post-processing is proposed in order to compute out of plane displacements due the relaxation of the residual stress profile obtained previously. In order to evaluate the influence of the run out table only, the final residual stress profile obtained at the end of the run out table (i.e., $x_3 = 140$) is applied on the whole 140 m long strip as though there were no subsequent evolution of the residual stress after the run out table (which is obviously not verified). A Finite Element simulation at finite strain is performed in order to quantify how residual stresses are relaxed by out of plane deformation. Thus, U_3 is not blocked any more and the tension is released. In figure 12 the residual stress profile after releasing the applied tension is presented. In comparison with figure 11 there is a clear relaxation of residual stresses through out of plane deformations. The out of plane displacement is presented in figure 13. It corresponds to the displacement that would occur if the strip were cut off just after the run out table. There is a *longbow* defect at both ends of the strip. Of course, the strip cooling continues during the coiling process and the residual stresses evolve as studied in [6–8].

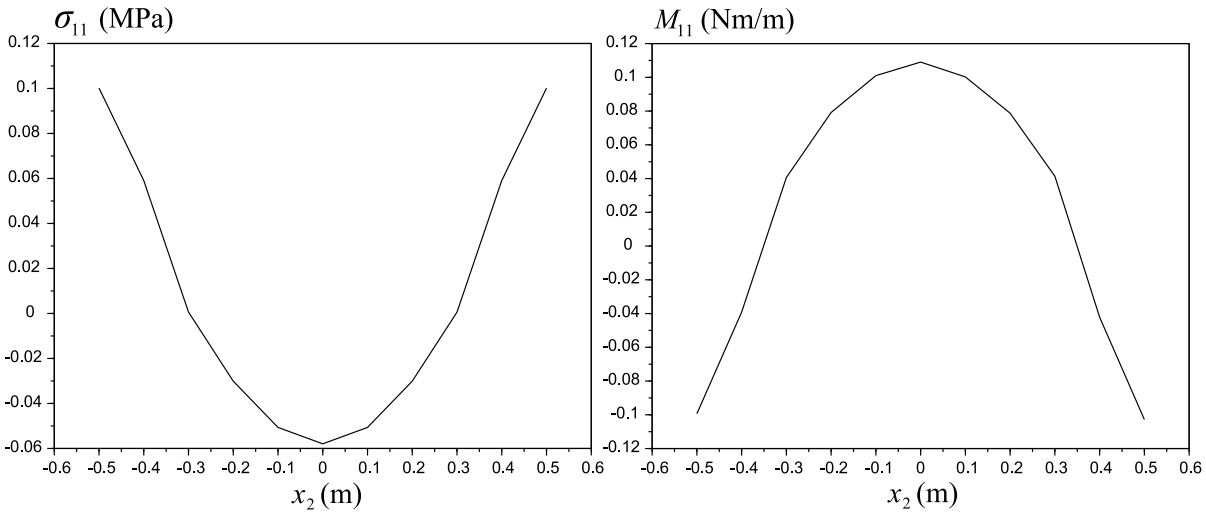

(a) Relaxed stress σ_{11} (b) Relaxed bending moment M_{11}

Figure 12: Relaxed stress profiles

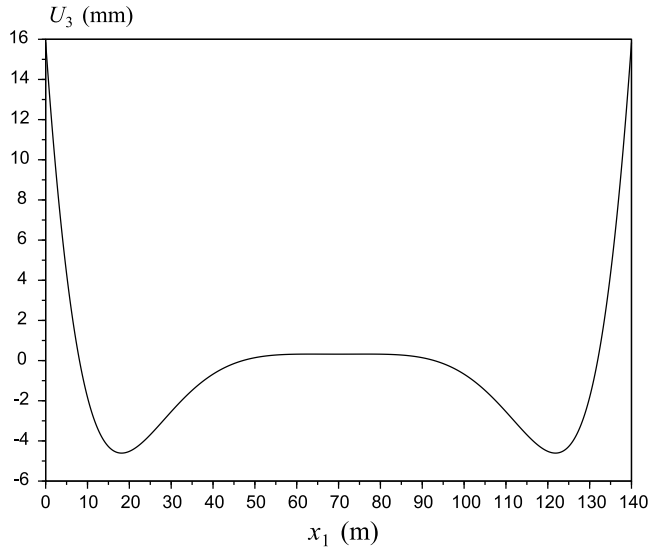

Figure 13: Out of pane displacement U_3

7. Conclusion

This contribution deals with a numerical strategy to simulate a non-linear and multiphysics problem: the cooling of a steel strip on the run out table. The proposed approach accounts for heat conduction strongly coupled with metallurgical transformations (multiphase transitions) and an elastic-plastic calculation of residual stress evolution. Thermal expansion, density mismatch between different phases and transformation induced plasticity are included under the form of an imposed increment of eigenstrain. This work enables to obtain reasonable computation times (around 2 hours for a 140 m long strip) because the mechanical problem is solved separately from the thermal/metallurgical problem and authorizing different meshing and time steps.

Numerical results show that homogenous cooling conditions along the strip width tend to decrease significantly the initial residual stress profile, but cooling one surface faster than the other creates an asymmetry that is responsible for bending moments. Therefore, classic flatness defects such as *longbow* and *crossbow* are detected.

8. Acknowledgements

Authors thank Didier Huin (ArcelorMittal) for their expertise and fruitful discussions.

References

[1] A. Hacquin, Modelisation thermo-mecanique tridimensionnelle du laminage: couplage bande-cylindres [3D thermomechanical modelling of rolling processes: coupling strip and rolls], Ph.D. thesis, Cemef Ecole des Mines de Paris, 1996. In French.

[2] P. Montmitonnet, Computer methods in applied mechanics and engineering 195 (2006) 6604–6625.

[3] X. Wang, Q. Yang, A. He, Journal of materials processing technology 207 (2008) 130–146.

[4] X. Wang, F. Li, Q. Yang, A. He, Applied Mathematical Modelling 37 (2013) 586–609.

[5] H.-H. Cho, Y.-G. Cho, D.-W. Kim, S.-J. Kim, W.-B. Lee, H. N. Han, ISIJ international 54 (2014) 1646–1652.

[6] D. Weisz-Patrault, A. Ehrlacher, N. Legrand, International Journal of Solids and Structures 94-95 (2016) 1–20.

[7] D. Weisz-Patrault, International Journal of Heat and Mass Transfer 104 (2017) 595–606.

[8] D. Weisz-Patrault, International Journal of Solids and Structures (2017). Submission.

[9] T. Waterschoot, B. De Cooman, D. Vanderschueren, Ironmaking & Steelmaking 28 (2001) 185–190.

[10] H. Yoshida, Transactions of the Iron and Steel Institute of Japan 24 (1984) 212–220.

[11] A. Kumar, C. McCulloch, E. Hawbolt, I. Samarasekera, Materials Science and Technology 7 (1991) 360–368.

[12] C.-G. Sun, H.-N. Han, J. Lee, Y.-S. Jin, S.-M. Hwang, ISIJ international 42 (2002) 392–400.

[13] S. Serajzadeh, Applied Mathematical Modelling 27 (2003) 861–875.

[14] S. Serajzadeh, Materials Science and Engineering: A 421 (2006) 260–267.

[15] M. H. Nasab, S. Serajzadeh, The International Journal of Advanced Manufacturing Technology 83 (2016) 1725–1736.

[16] M. Avrami, The Journal of Chemical Physics 7 (1939) 1103–1112.

[17] H. N. Han, J. K. Lee, H. J. Kim, Y.-S. Jin, Journal of Materials Processing Technology 128 (2002) 216–225.

[18] Z. Zhou, P. F. Thomson, Y. Lam, D. D. Yuen, Journal of Materials Processing Technology 132 (2003) 184–197.

[19] U. M. Abaqus, Abaqus, 2006.

[20] T. Iung, M. Kandel, D. Quidort, Y. De Lassat, Revue de Métallurgie–International Journal of Metallurgy 100 (2003) 173–181.

[21] A. Perlade, D. Grandemange, T. Iung, Ironmaking & steelmaking 32 (2005) 299–302.

[22] D. Huin, D. Grandemange, P. Maugis, G. Herman, in: International Conference on Thermomechanical Processing of Steels–TMP, pp. 1–12.

[23] Scilab, Scilab Enterprises, Orsay, France (2012).

[24] CEA, Cast3m, 2011. Commissariat a l'Energie Atomique, http://www-cast3m.cea.fr/.

[25] J. W. Cahn, Acta Metallurgica 4 (1956) 449–459.

[26] Y.-T. Pan, Measurement and Modelling of Diffusional Transformation of Austenite in C-Mn Steels, Ph.D. thesis, National Sun Yat-Sen University, 2001.

[27] J.-B. Leblond, G. Mottet, J. Devaux, Journal of the Mechanics and Physics of Solids 34 (1986) 395–409.

[28] J.-B. Leblond, G. Mottet, J. Devaux, Journal of the Mechanics and Physics of Solids 34 (1986) 411–432.

[29] J.-B. Leblond, J. Devaux, J. Devaux, International journal of plasticity 5 (1989) 551–572.

[30] J.-B. Leblond, International journal of plasticity 5 (1989) 573–591.

[31] L. Taleb, F. Sidoroff, International Journal of Plasticity 19 (2003) 1821–1842.

[32] H. N. Han, J. K. Lee, ISIJ international 42 (2002) 200–205.

[33] M.-G. Lee, S.-J. Kim, H. N. Han, W. C. Jeong, International Journal of Plasticity 25 (2009) 1726–1758.

[34] D. Weisz-Patrault, Journal of the Mechanics and Physics of Solids (2017).

[35] M. Martinez, Jonction 16 MND 5-Inconel 690-316 LN par soudage-diffusion: élaboration et calcul des contraintes résiduelles de procédé, Ph.D. thesis, ENSMP, 1999.

[36] SYSWELD®, Esi group, france, 2012.

Figure

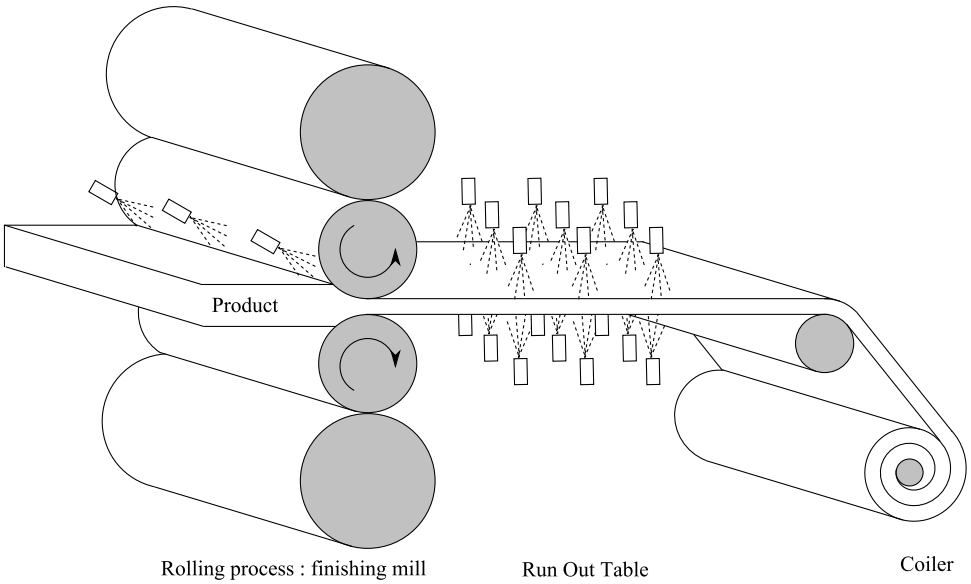

Figure 1: Chain of hot forming processes

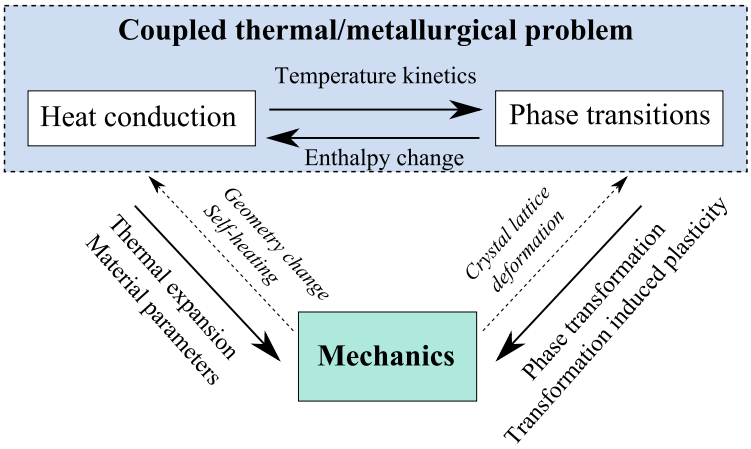

Figure 2: Couplings

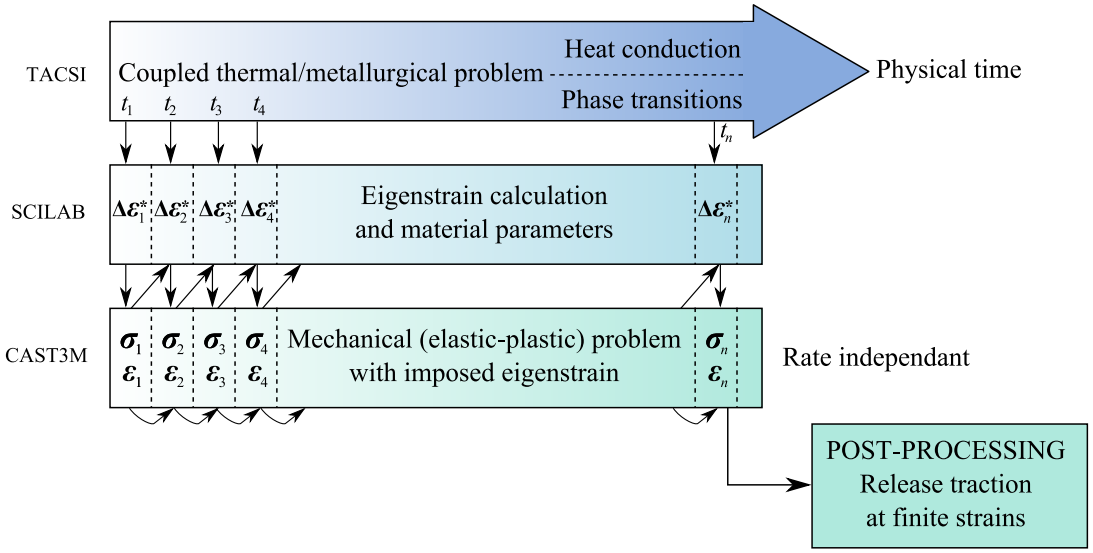

Figure 3: Numerical scheme

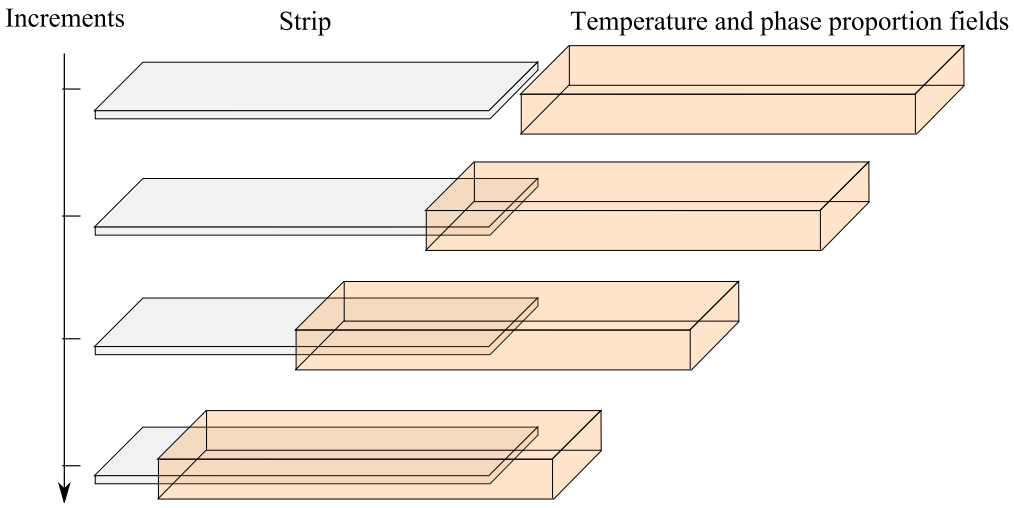

Figure 4: History of mechanical states

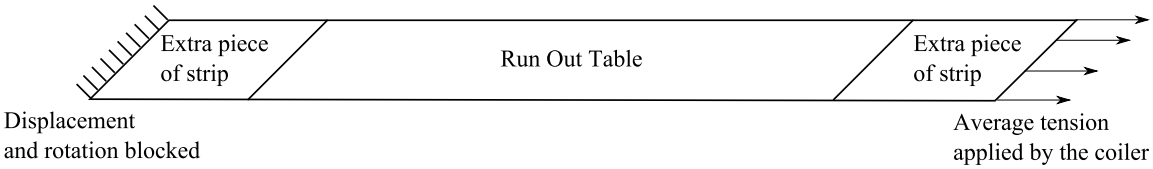

Figure 5: Boundary conditions

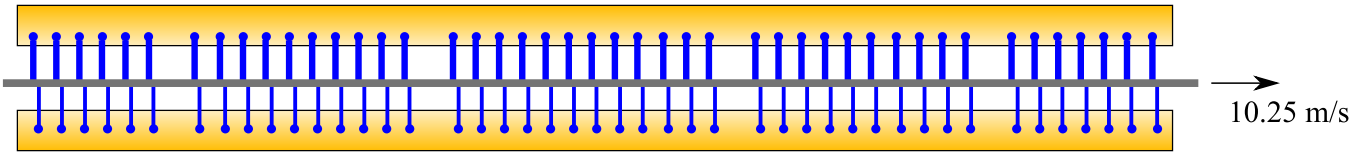

Figure 6: Prescribed cooling path

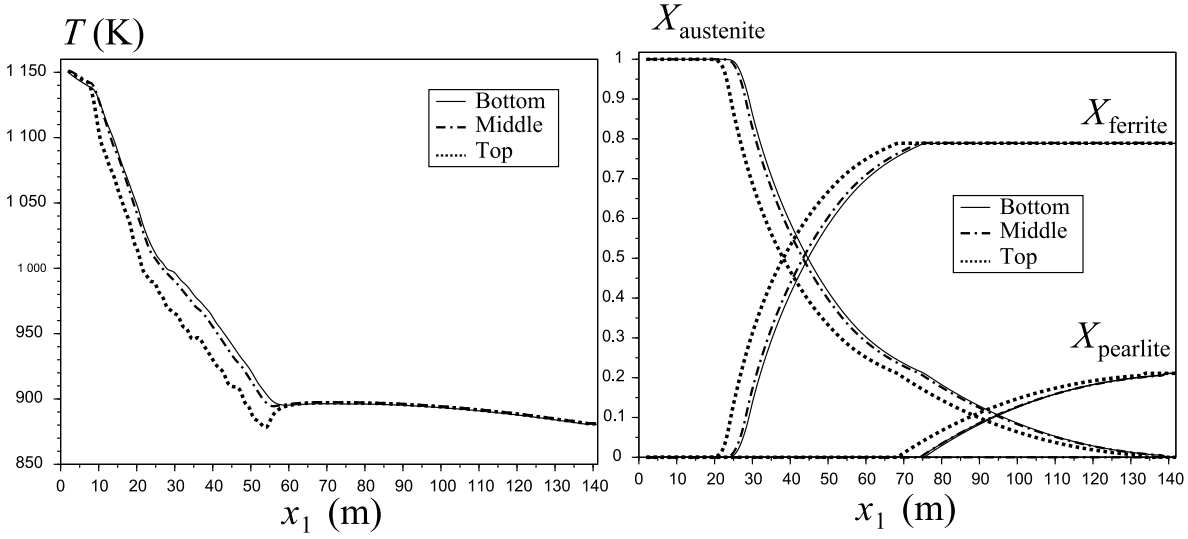

(a) Temperature field

(b) Phase proportion field

Figure 7: Coupled thermal/metallurgical problem

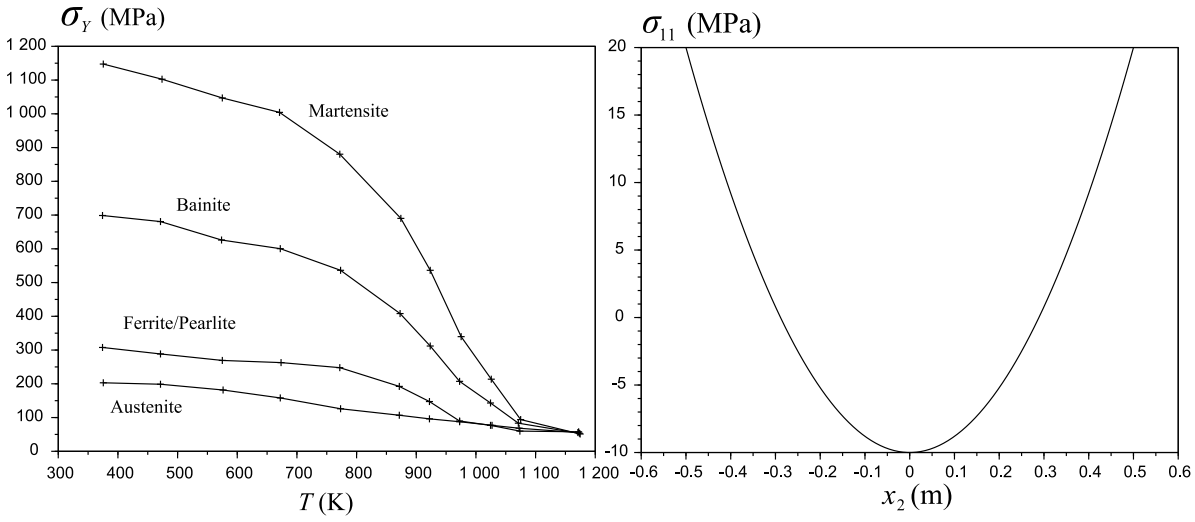

(a) Yield stress of each phase

(b) Initial residual stress profile

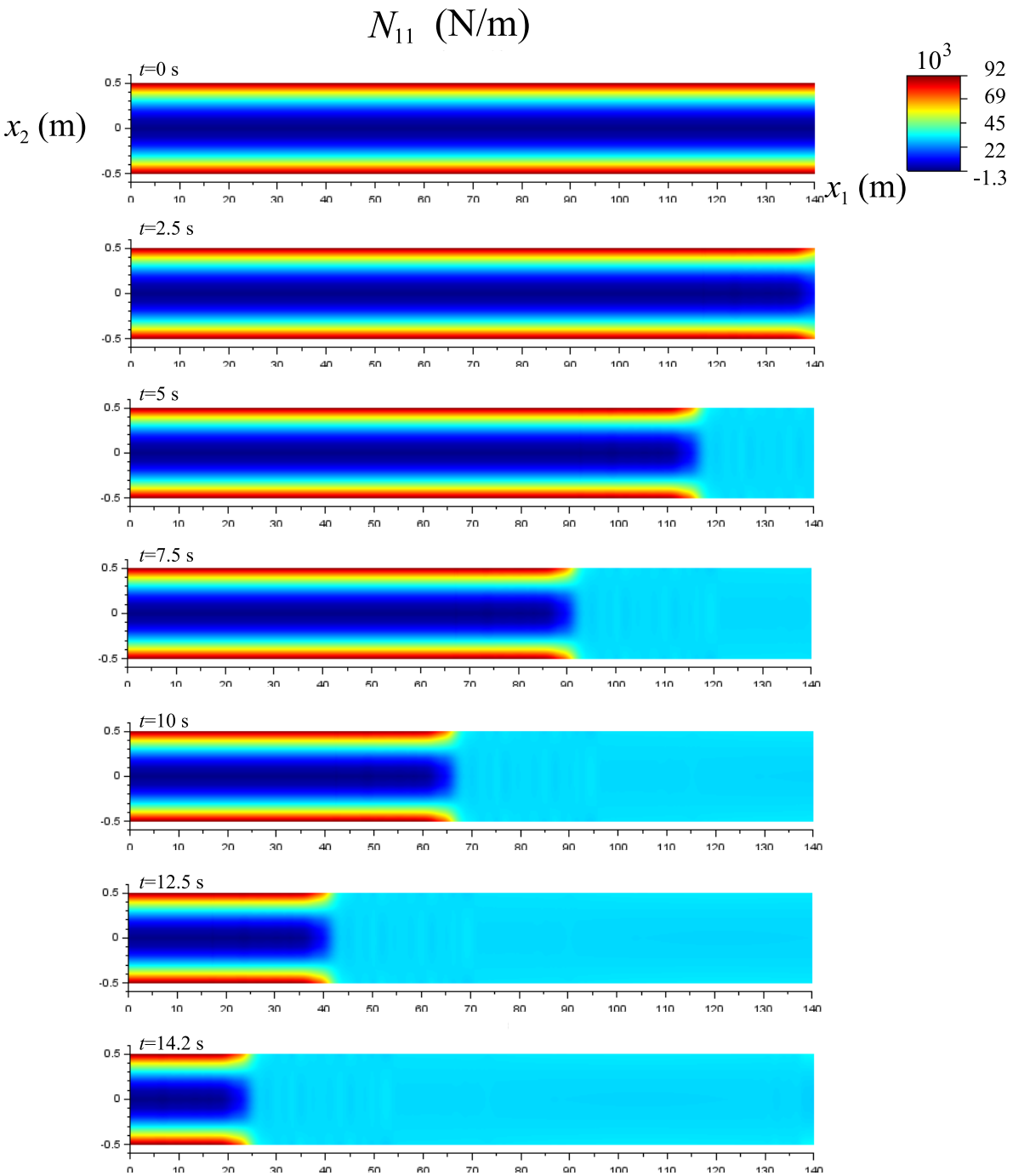

Figure 9: In-plane stress resultant N_{11}

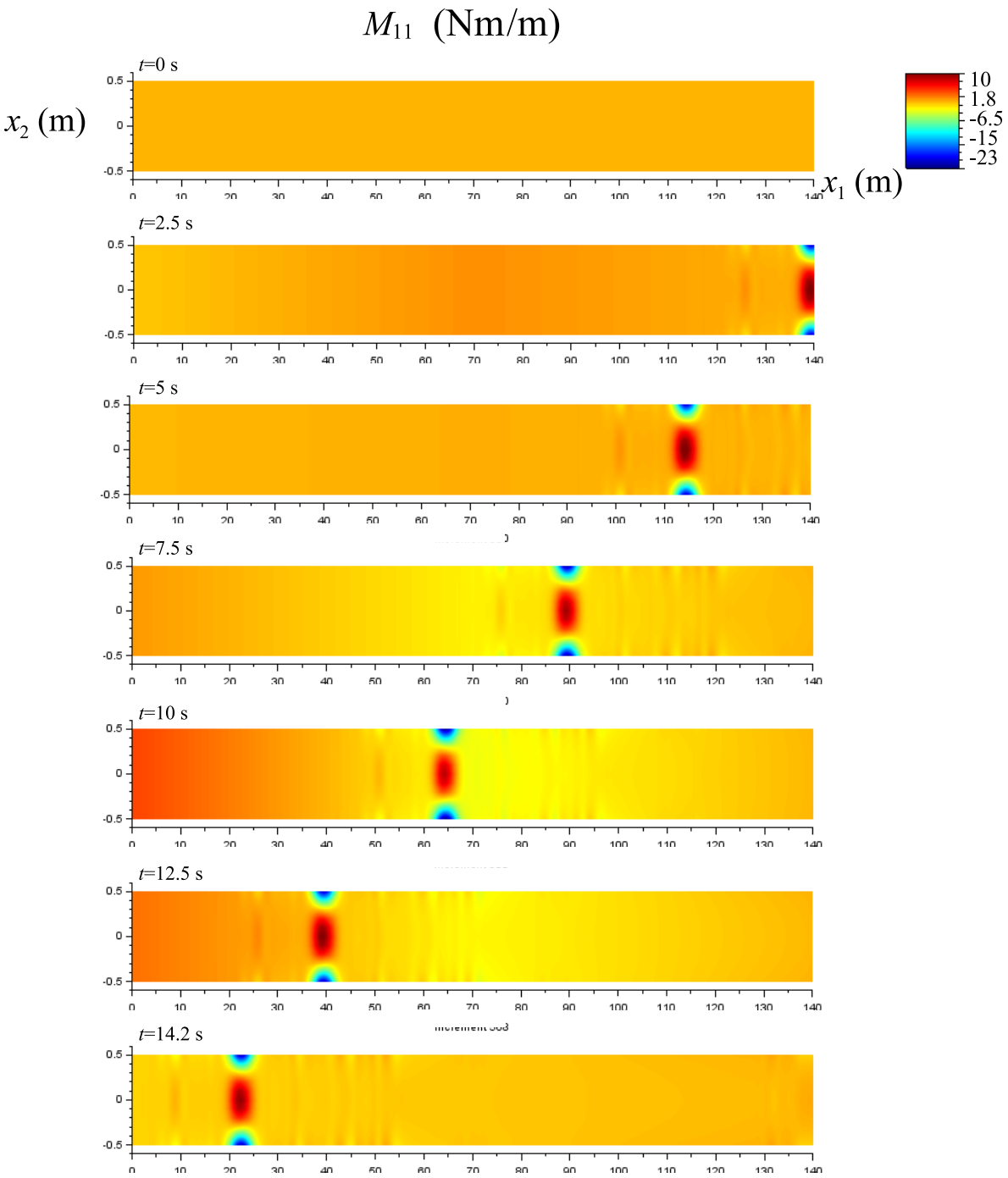

Figure 10: Bending moment M_{11}

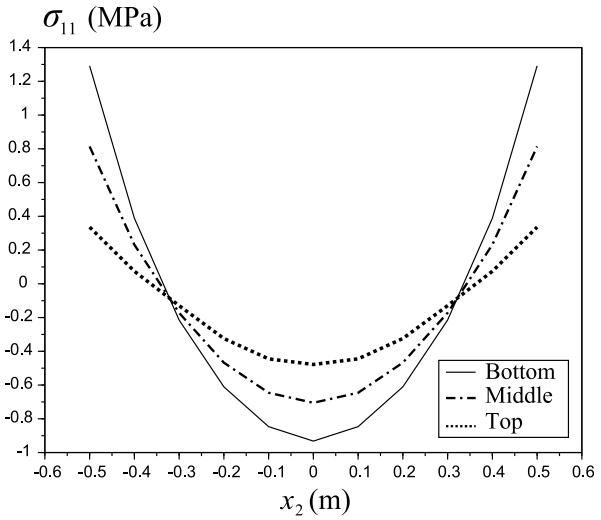

(a) Final residual stress σ_{11}

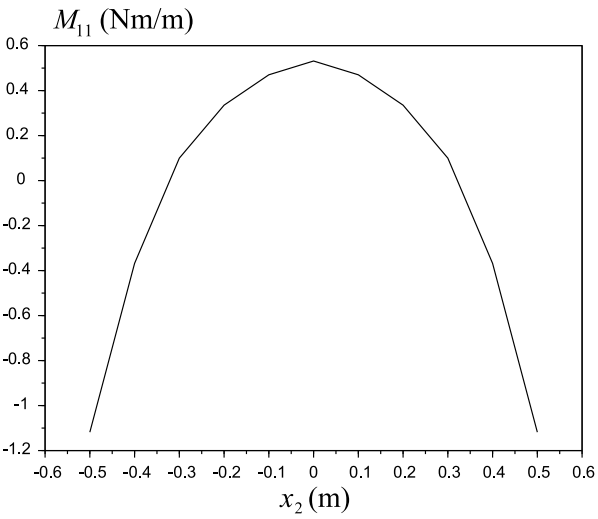

(b) Final bending moment M_{11}

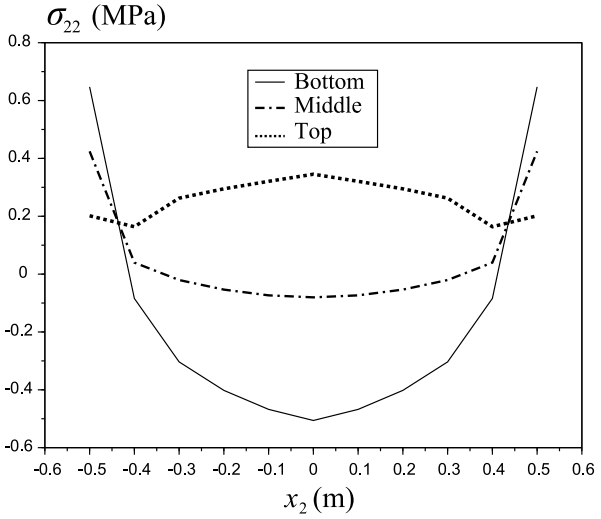

(c) Final residual stress σ_{22}

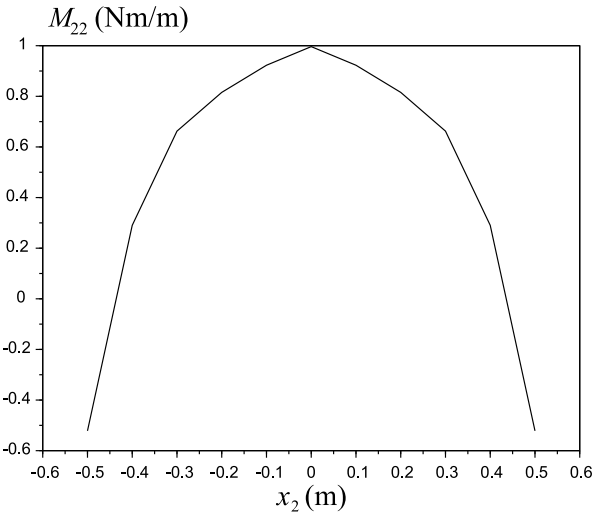

(d) Final bending moment M_{22}

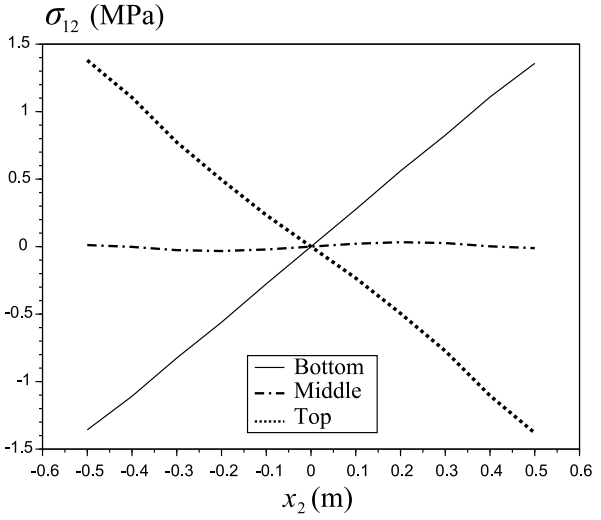

(e) Final residual stress σ_{12}

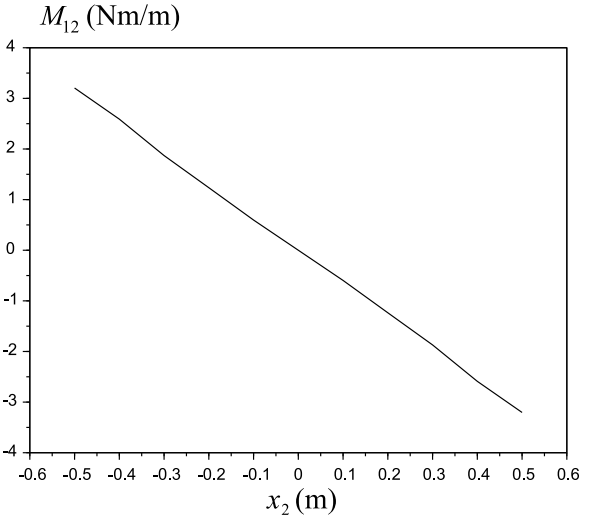

(f) Final bending moment M_{12}

Figure 11: Final stress profiles

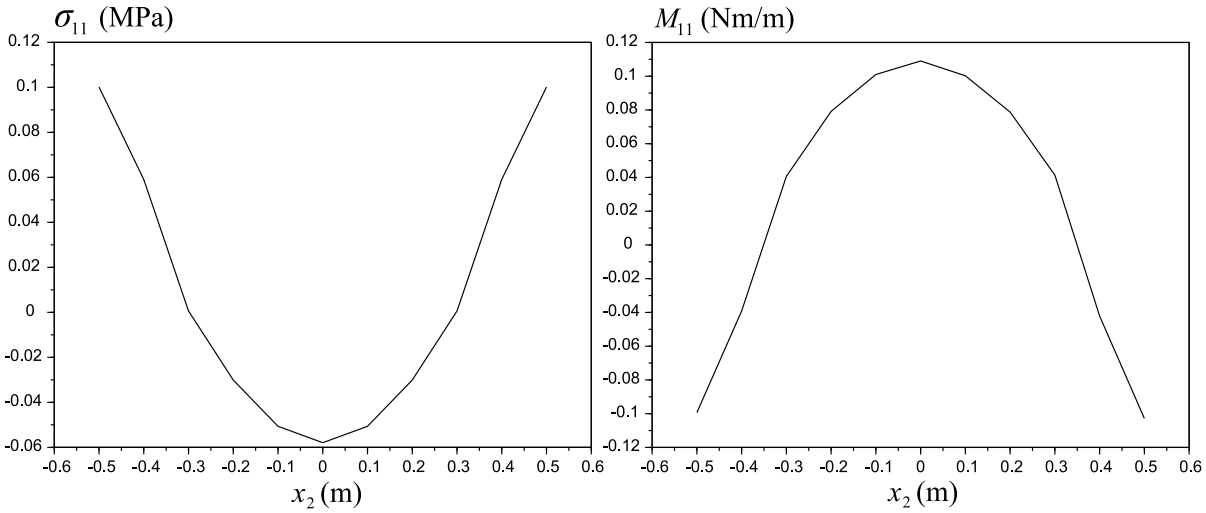

(a) Relaxed stress σ_{11} (b) Relaxed bending moment M_{11}

Figure 12: Relaxed stress profiles

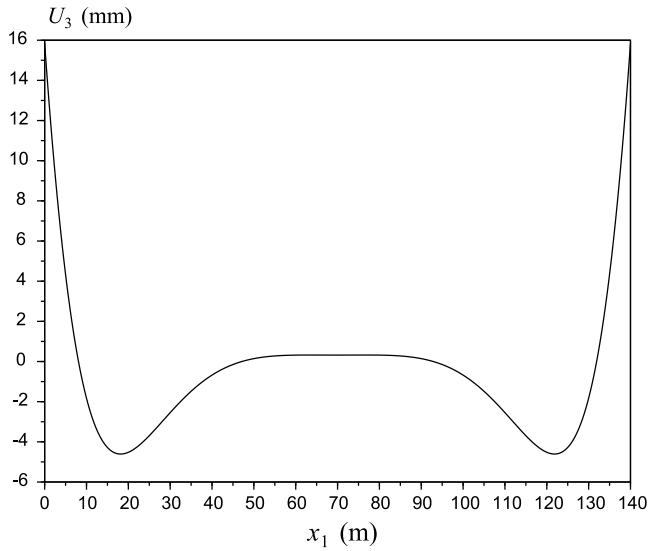

Figure 13: Out of pane displacement U_3